

An anelliptic approximation for geometric spreading in transversely isotropic and orthorhombic media

Shibo Xu¹, Alexey Stovas¹, and Yanadet Sripanich²

ABSTRACT

The relative geometric spreading along the raypath contributes to the amplitude decay of the seismic wave propagation that needs to be considered for amplitude variation with offset or other seismic data processing methods that require the true amplitude processing. Expressing the P-wave geometric spreading factor in terms of the offset-traveltime-based parameters is a more practical and convenient way because these parameters can be estimated from the nonhyperbolic velocity analysis. We have developed an anelliptic approximation for the relative geometric spreading of P-wave in a homogeneous transversely isotropic medium with vertical symmetry axis (VTI) and an orthorhombic (ORT) medium under the acoustic anisotropy assumption. The coefficients in

our approximation are only defined within the symmetry planes and computed from fitting with the exact parametric expression. For an ORT model, due to the symmetric behavior in different symmetry planes, the other coefficients in the approximation can be easily obtained by making corresponding changes in indices from the computed coefficients in one symmetry plane. From the numerical examples, we found that for a homogeneous VTI model, the anelliptic approximation is more accurate than the generalized nonhyperbolic moveout approximation form for larger offset. For a homogeneous ORT model, our anelliptic approximation is more accurate than its traveltime-based counterparts. Using the Dix-type equations for the effective parameters, our anelliptic form approximation is extended to a multilayered VTI and ORT models and has accurate results in both models.

INTRODUCTION

Geometric spreading describes the amplitude decay of propagating waves and is one of the most fundamental subjects in seismic data processing. It is important for prestack Kirchhoff's migration, amplitude variation with offset (AVO) analysis, and other seismic data processing methods that require true amplitude processing. The amplitude distribution along the wavefront of the reflected wave is changed greatly if the velocity model is anisotropic. Seismic data must be compensated for geometric spreading before AVO or amplitude versus angle analysis to study reflection coefficients as a function of offset or incidence angle. Although geometric spreading is a dynamic quantity, it is governed by the kinematic parameters of seismic waves. When the velocity model is available, relative geometric spreading can be computed by performing dynamic ray tracing. However, accurate information about the anisotropic velocity model for the whole overburden is seldom available for practice. To

avoid the use of numerical ray tracing, expressing geometric spreading through traveltime of the reflection events recorded at the surface using ray theory (Červený, 2001) is a more practical method for seismic time processing. Therefore, it is convenient to express geometric spreading in terms of the offset-traveltime parameters that can be estimated from the nonhyperbolic velocity analysis.

Ursin (1990) proposes a geometric spreading approximation represented by traveltime parameters for a layered isotropic medium. One of the practical contributions from the paraxial ray theory is an expression for geometric spreading in terms of the traveltime functions at the source and receiver locations (Červený, 2001). Zhou and McMechan (2000) derive an analytical formula for the geometric spreading of P waves in a layered transversely isotropic medium with vertical symmetry axis (VTI) with the source and receivers in the same layer. Ursin and Hokstad (2003) extend the method of Ursin (1990) for multiple reflected and converted P- and SV-waves in a layered VTI medium with the source and receivers in different

Manuscript received by the Editor 16 January 2017; revised manuscript received 9 July 2017; published ahead of production 03 October 2017; published online 14 November 2017.

¹Norwegian University of Science and Technology, Department of Geoscience and Petroleum, Trondheim, Norway. E-mail: shibo.xu@ntnu.no; alexey.stovas@ntnu.no.

²The University of Texas at Austin, Bureau of Economic Geology, Austin, Texas, USA. E-mail: yanadet.sripanich@gmail.com.

© 2018 Society of Exploration Geophysicists. All rights reserved.

layers. For pure reflection modes (P or SV) in layered anisotropic media, the geometric spreading as a function of traveltimes was obtained by Xu et al. (2005). The geometric spreading correction for an azimuthally anisotropic medium was later derived by Xu and Tsvankin (2006), and it was extended for converted waves in a VTI medium (Xu and Tsvankin, 2008). A practical application of anisotropic geometric spreading for AVO analysis was made by Xu and Tsvankin (2007), with the wide-azimuthal data acquired at Rulison Field, Colorado. The traveltimes-based geometric spreading approximation in transversely isotropic medium with tilted symmetry axis (TTI) media is derived by Golikov and Stovas (2013). All of these approximations are approximating the traveltimes and use it and its derivatives for computation of the geometric spreading approximation. We refer to it as traveltimes-based approximation or indirect approximation. Different nonhyperbolic moveout approximations for a homogeneous VTI model are listed in Fowler (2003) and Golikov and Stovas (2012). Although the geometric spreading factor is controlled by first- and second-order traveltimes derivatives, there is no guarantee that the most accurate traveltimes approximation being used in equations for geometric spreading results in the most accurate geometric spreading equation. Different from the indirect type approximation, which is approximating the traveltimes for geometric spreading approximation, the direct-type approximation is computed by approximating the geometric spreading term directly from the exact parametric equations obtained from dynamic ray tracing. The first example of this comparison between indirect and direct type approximation is done by Stovas and Ursin (2009), who developed the rational type of approximation in direct form. They showed that the direct rational approximation is simpler and more accurate than the indirect counterpart for a homogeneous and multilayered VTI model. Xu and Stovas (2017) propose a direct type approximation with the generalized nonhyperbolic form (Fomel and Stovas, 2010) for the relative geometric spreading for a VTI medium and compared them with indirect ones.

The orthorhombic (ORT) model is introduced by Schoenberg and Helbig (1997) and has gained more attention due to the need to characterize the fractured earth. They have become a new standard to define model parameters to cover the azimuthal dependence of the traveltimes surface. Tsvankin (1997, 2012) defines nine elastic model parameters for an ORT model that can be reduced to six parameters in an acoustic approximation (Alkhalifah, 2003). In the group domain, we refer to the first-order curvature as the normal moveout (NMO) velocity ellipses (Grechka and Tsvankin, 1999a, 1999b) and the second-order curvature as the anellipticities because they represent the anelliptic behavior for slowness and the traveltimes surface. Stovas (2015) derives azimuthally dependent kinematic properties of ORT media and defines the effective ORT parameters in the Dix-type in layered ORT media that derived from the Dix (1955) inversion. Sripanich and Fomel (2015) modify the anelliptic functional form of Fomel (2004) and extend it to an ORT model to approximate P-wave phase and group velocities.

In this paper, we propose an anelliptic approximation in reminiscent of the functional form studied by Sripanich and Fomel (2015) for direct-type relative geometric spreading in VTI and ORT media. The coefficients in the approximation are defined within the symmetry plane and obtained from fitting with exact relative geometric spreading in the symmetry planes. Due to the symmetric behavior in different symmetry planes by using the acoustic anisotropy assumption

(Alkhalifah, 1998), the computation for the coefficients in ORT model becomes easier by applying the corresponding changes in the forms of the coefficients that are obtained in one symmetry plane. Subsequently, we extend our method for layered VTI and ORT models by using the effective model parameters computed from the Dix-type equation (Stovas, 2015). Using numerical examples, we show that the results from our approximation are highly accurate for homogeneous and layered VTI and ORT cases.

RELATIVE GEOMETRIC SPREADING IN A VTI MODEL

The relative geometric spreading is given in Červený (2001) as

$$\mathcal{L} = \sqrt{\frac{\cos \theta_S \cos \theta_R}{|\det \mathbf{M}|}}, \quad (1)$$

where θ_S and θ_R are the angles between the ray and the normal to the surface measured at the source and receiver, respectively. Measured from the dynamic ray tracing, θ_S and θ_R are all group angle. \mathbf{M} is the second-order derivatives of the traveltimes (T) matrix given by

$$\mathbf{M} = \begin{pmatrix} \frac{\partial^2 T}{\partial x_S \partial x_R} & \frac{\partial^2 T}{\partial x_S \partial y_R} \\ \frac{\partial^2 T}{\partial y_S \partial x_R} & \frac{\partial^2 T}{\partial y_S \partial y_R} \end{pmatrix}, \quad (2)$$

where (x_S, y_S) and (x_R, y_R) are the lateral coordinates of source and receiver, respectively. The relative geometric spreading in a VTI model is given by (Ursin and Hokstad, 2003)

$$\mathcal{L} = \Omega \left(\frac{1}{x} \frac{dt}{dx} \right)^{-1/2} \left(\frac{d^2 t}{dx^2} \right)^{-1/2}, \quad (3)$$

where Ω is the radiation pattern given by $\Omega = \sqrt{\cos \theta_S \cos \theta_R}$. In this paper, we neglect the radiation pattern and focus only on the term \mathcal{L}_N that is given as

$$\mathcal{L}_N = \left(\frac{1}{x} \frac{dt}{dx} \frac{d^2 t}{dx^2} \right)^{-1/2}. \quad (4)$$

The relative geometric spreading term \mathcal{L}_N given in equation 4 can also be written as a function of horizontal slowness p in the case of flat layer as follows (Stovas and Ursin, 2009):

$$\mathcal{L}_N = \left(\frac{x}{p} \frac{dx}{dp} \right)^{1/2}. \quad (5)$$

For a homogeneous VTI model, the offset under an acoustic approximation can be given in terms of horizontal slowness Alkhalifah (1998):

$$x(p) = \frac{p t_0 V_n^2}{(1 - 2\eta p^2 V_n^2)^{3/2} \sqrt{1 - (1 + 2\eta) p^2 V_n^2}}, \quad (6)$$

where t_0 is the vertical one-way traveltimes, V_n is the NMO velocity, and η is the anellipticity parameter (Alkhalifah, 1998). Substituting equation 6 into equation 5 gives (Stovas and Ursin, 2009)

$$\mathcal{L}_N = \frac{t_0 V_n^2 \sqrt{1 + 4\eta p^2 V_n^2 - 6\eta(1 + 2\eta)p^4 V_n^4}}{(1 - 2\eta p^2 V_n^2)^2 (1 - (1 + 2\eta)p^2 V_n^2)}. \quad (7)$$

Equations 6 and 7 give an exact parametric equation for relative geometric spreading \mathcal{L}_N in terms of the horizontal slowness that can be measured from dynamic ray tracing.

Anelliptic form approximation for the relative geometric spreading in a VTI model

In VTI medium, we define the approximation for the relative geometric spreading in an anelliptic resembling that of [Sripanich and Fomel \(2015\)](#) by

$$\mathcal{L}_N = h(1 - \hat{s}) + \hat{s} \sqrt{h^2 + \frac{2(\hat{q} - 1)w_1 w_3 x^2}{\hat{s}}}, \quad (8)$$

where the hyperbolic term $h = h(x)$ denotes the elliptic part of the relative geometric spreading given by

$$h = w_1 x^2 + w_3, \quad (9)$$

with

$$\begin{aligned} w_1 &= \lim_{x \rightarrow \infty} \frac{\mathcal{L}_N}{x^2} = \frac{1}{t_0 \sqrt{1 + 2\eta}}, \\ w_3 &= \lim_{x \rightarrow 0} \mathcal{L}_N = t_0 V_n^2. \end{aligned} \quad (10)$$

The functions $\hat{q} = \hat{q}(x)$ and $\hat{s} = \hat{s}(x)$ are defined by

$$\begin{aligned} \hat{q} &= \frac{q_1 w_1 x^2 + q_3 w_3}{h}, \\ \hat{s} &= \frac{s_1 w_1 x^2 + s_3 w_3}{h}, \end{aligned} \quad (11)$$

where $q_1, q_3, s_1,$ and s_3 are the coefficients computed from the fitting process with the exact geometric spreading form. Note that w_1 and w_3 in equation 9 have different units. If we define the hyperbolic term by $h = w_1 x^2 + w_3 t_0^2 V_0^2$, where V_0 is the vertical velocity, they will have the same units. The reason why we do not use this form is that we do not have vertical velocity in our list of parameters.

The offset and the depth is shown by the relation $x = z \tan(\theta)$, where z is the depth and θ is the dip group angle from the vertical axis. We define a function $r = r(\theta)$ that relates to the relative geometric spreading as

$$r = \frac{\cos(\theta)^2 \mathcal{L}_N(x = z \tan(\theta))}{z^2}. \quad (12)$$

The coefficients $q_1, q_3, s_1,$ and s_3 in equation 8 can be computed by fitting with the exact equation for \mathcal{L}_N (see equation A-3) through the second- ($\partial^2 r / \partial \theta^2$) and fourth-order derivatives $\partial^4 r / \partial \theta^4$ at $\theta = 0^\circ$ and 90° , as noted by indices 1 and 3 for the horizontal and vertical axes, respectively (Figure 1). The equations for $q_1, q_3, s_1,$ and s_3 are given in Appendix A.

The coefficients $q_1, q_3, s_1,$ and s_3 are plotted versus anellipticity parameter η in Figure 2. The coefficients q_1 and q_3 are gradually increasing with η , whereas s_1 and s_3 are almost independent of η .

When setting $\eta = 0$ corresponding to elliptical anisotropy, they become equivalent to each other with $q_1 = q_3 = 1$ and $s_1 = s_3 = 9/13$.

To test the accuracy of the anelliptic approximation, we use a homogeneous VTI model with parameters: $t_0 = 1$ s, $V_n = 2$ km/s, and $\eta = 0.2$. We show the relative error in relative geometric spreading versus normalized offset computed from our method and the approximation in generalized nonhyperbolic moveout approximation (GMA) form approximation computed from infinite offset limit ([Xu et al., 2016](#)) in Figure 3. Note that the approximations are compared with the exact parametric expression shown in equations 6 and 7 that are computed from dynamic ray tracing. One can see that comparing with GMA form approximation in a homogeneous VTI model, the anelliptic approximation is less accurate at a short offset, whereas when approaching a larger offset, it becomes more accurate since the fixed elliptical background is used. Subsequently, we introduce a

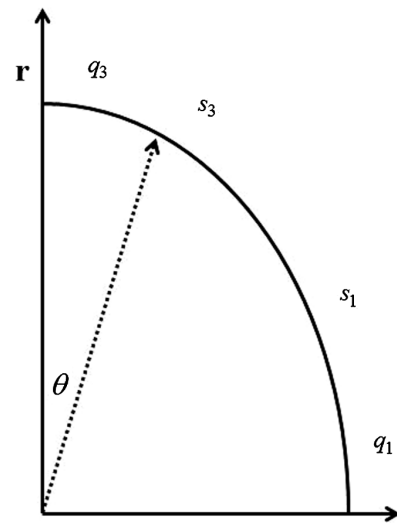


Figure 1. The location of fitting indices $q_1, q_3, s_1,$ and s_3 in a homogeneous VTI model.

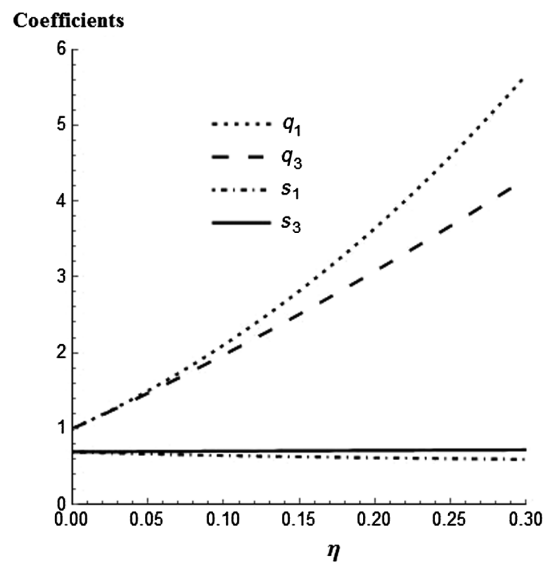


Figure 2. The sensitivity of coefficients $q_1, q_3, s_1,$ and s_3 versus anellipticity η .

multilayered VTI model using the parameters in Table 1 and show the relative error versus offset-depth ratio in Figure 4. The effective model parameters are computed from Dix-type equations shown in Appendix B. One can see that the errors are all increasing with η , and the error from the anelliptic approximation is always smaller than the GMA form approximation.

RELATIVE GEOMETRIC SPREADING IN A HOMOGENEOUS ORT MODEL

For a homogeneous ORT model, we introduce two lateral offset projections:

$$\begin{aligned} x &= x_R - x_S, \\ y &= y_R - y_S. \end{aligned} \quad (13)$$

The matrix \mathbf{M} in equation 2 takes the form:

$$\mathbf{M} = \begin{pmatrix} \frac{\partial^2 T}{\partial x^2} & \frac{\partial^2 T}{\partial x \partial y} \\ \frac{\partial^2 T}{\partial y \partial x} & \frac{\partial^2 T}{\partial y^2} \end{pmatrix}. \quad (14)$$

In the phase domain, the relative geometric spreading \mathcal{L}_N can be given by Stovas (2017):

$$\mathcal{L}_N = \left(\frac{\partial x}{\partial p_x} \frac{\partial y}{\partial p_y} - \frac{\partial y}{\partial p_x} \frac{\partial x}{\partial p_y} \right)^{1/2}. \quad (15)$$

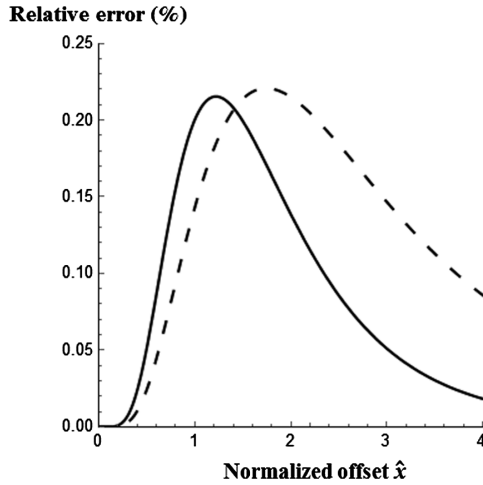


Figure 3. The relative error for anelliptic (solid) and GMA form (dashed) approximation for the relative geometric spreading in a homogeneous VTI medium.

Table 1. The model parameters in a multilayered VTI model.

Layer	Layer thickness (km)	Vertical velocity (km/s)	NMO velocity (km/s)	Anellipticity parameter
1	0.3	1.5	1.8	0.1
2	0.7	1.8	2	0.15
3	1	2	2.2	0.18

To compute the geometric spreading for a homogeneous ORT model, we use exact parametric offset equations (Stovas, 2015):

$$\begin{aligned} x(p_x, p_y) &= p_x F_2^2 \frac{V_{n1}^2 t_0}{f_1^{1/2} f_2^{3/2}}, \\ y(p_x, p_y) &= p_y F_1^2 \frac{V_{n2}^2 t_0}{f_1^{1/2} f_2^{3/2}}, \end{aligned} \quad (16)$$

where $x(p_x, p_y)$ and $y(p_x, p_y)$ are the corresponding offset projections, and

$$\begin{aligned} F_1 &= 1 - p_x^2 V_{n1}^2 (2\eta_1 - \eta_{xy}), \\ F_2 &= 1 - p_y^2 V_{n2}^2 (2\eta_2 - \eta_{xy}), \\ f_1 &= 1 - (1 + 2\eta_1) p_x^2 V_{n1}^2 - (1 + 2\eta_2) p_y^2 V_{n2}^2 \\ &\quad + ((1 + 2\eta_1)(1 + 2\eta_2) - (1 + \eta_{xy})^2) p_x^2 p_y^2 V_{n1}^2 V_{n2}^2, \\ f_2 &= 1 - 2\eta_1 p_x^2 V_{n1}^2 - 2\eta_2 p_y^2 V_{n2}^2 + (4\eta_1 \eta_2 - \eta_{xy}^2) p_x^2 p_y^2 V_{n1}^2 V_{n2}^2, \end{aligned} \quad (17)$$

where V_{n1} and V_{n2} are the corresponding NMO velocities defined in $[X, Z]$ and $[Y, Z]$ planes, respectively. Anellipticity parameters η_1 and η_2 are defined in corresponding two vertical symmetry $[X, Z]$ and $[Y, Z]$ planes, respectively. Note that the definition of indices is different with the one defined in standard Tsvankin (1997) indices. The cross-term anellipticity parameter η_{xy} is defined as (Stovas, 2015)

$$\eta_{xy} = \sqrt{\frac{(1 + 2\eta_1)(1 + 2\eta_2)}{1 + 2\eta_3}} - 1, \quad (18)$$

where anellipticity parameter η_3 is defined in the $[X, Y]$ plane (Vasconcelos and Tsvankin, 2006).

The relative geometric spreading for ORT medium is given by Stovas (2017)

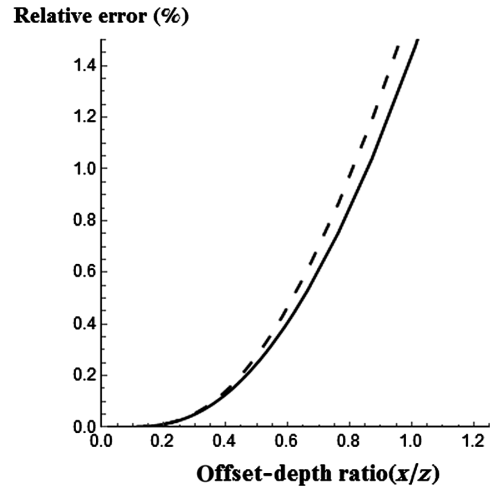


Figure 4. The relative error for anelliptic (solid) and GMA form (dashed) approximation for the relative geometric spreading in a multilayered VTI medium.

$$\mathcal{L}_N = t_0 V_{n1} V_{n2} \frac{F_1 F_2}{f_2^2 f_1} \sqrt{f_m}, \quad (19)$$

where

$$\begin{aligned} f_m = & 1 + 4\eta_1 p_x^2 V_{n1}^2 + 4\eta_2 p_y^2 V_{n2}^2 - 6\eta_1(1 + 2\eta_1) p_x^4 V_{n1}^4 \\ & - 6\eta_2(1 + 2\eta_2) p_y^4 V_{n2}^4 \\ & + 2(8\eta_1\eta_2 - \eta_{xy}(3 + 5\eta_{xy})) p_x^2 p_y^2 V_{n1}^2 V_{n2}^2 \\ & - 6(1 + 2\eta_1)(4\eta_1\eta_2 - \eta_{xy}^2) p_x^4 p_y^2 V_{n1}^4 V_{n2}^2 - 6(1 + 2\eta_2) \\ & \times (4\eta_1\eta_2 - \eta_{xy}^2) p_x^2 p_y^4 V_{n1}^2 V_{n2}^4 \\ & + 9((1 + 2\eta_1)(1 + 2\eta_2) - (1 + \eta_{xy})^2)(4\eta_1\eta_2 - \eta_{xy}^2) \\ & \times p_x^4 p_y^4 V_{n1}^4 V_{n2}^4. \end{aligned} \quad (20)$$

Anelliptic approximation for the relative geometric spreading in an ORT model

In ORT medium, we define the approximation for relative geometric spreading in an anelliptic form similar to [Sripanich and Fomel \(2015\)](#)

$$\mathcal{L}_{N(\text{ORT})} = H(1 - \hat{S}) + \hat{S} \sqrt{H^2 + F}, \quad (21)$$

with

$$\begin{aligned} F = & F(x, y) \\ = & \frac{2((\hat{Q}_1 - 1)W_2 W_3 y^2 + (\hat{Q}_2 - 1)W_1 W_3 x^2 + (\hat{Q}_3 - 1)W_1 W_2)}{\hat{S}}, \end{aligned} \quad (22)$$

where the hyperbolic term $H = H(x, y)$ denotes the elliptic part of the relative geometric spreading given by

$$H = W_1 x^2 + W_2 y^2 + W_3, \quad (23)$$

with

$$\begin{aligned} W_1 = & \lim_{x \rightarrow \infty, y \rightarrow 0} \frac{\mathcal{L}_{N(\text{ORT})}}{x^2} = \frac{(1 + \eta_{xy})V_{n2}}{t_0(1 + 2\eta_1)^{3/2}V_{n1}}, \\ W_2 = & \lim_{x \rightarrow 0, y \rightarrow \infty} \frac{\mathcal{L}_{N(\text{ORT})}}{y^2} = \frac{(1 + \eta_{xy})V_{n1}}{t_0(1 + 2\eta_2)^{3/2}V_{n2}}, \\ W_3 = & \lim_{x \rightarrow 0, y \rightarrow 0} \mathcal{L}_N(\text{ORT}) = t_0 V_{n1} V_{n2}. \end{aligned} \quad (24)$$

The functions $\hat{Q}_i = \hat{Q}_i(x, y)$, ($i = 1, 2, 3$) are defined as

$$\begin{aligned} \hat{Q}_1(x, y) = & \frac{Q_{21}W_2 y^2 + Q_{31}W_3}{W_2 y^2 + W_3}, \\ \hat{Q}_2(x, y) = & \frac{Q_{12}W_1 x^2 + Q_{32}W_3}{W_1 x^2 + W_3}, \\ \hat{Q}_3(x, y) = & \frac{Q_{13}W_1 x^2 + Q_{23}W_2 y^2}{W_1 x^2 + W_2 y^2}. \end{aligned} \quad (25)$$

The function $\hat{S} = \hat{S}(x, y)$ is given by

$$\hat{S}(x, y) = \frac{\hat{S}_1(x, y)W_1 x^2 + \hat{S}_2(x, y)W_2 y^2 + \hat{S}_3(x, y)W_3}{H}, \quad (26)$$

where

$$\begin{aligned} \hat{S}_1(x, y) = & \frac{S_{13}W_2 y^2 + S_{12}W_3}{W_2 y^2 + W_3}, \\ \hat{S}_2(x, y) = & \frac{S_{23}W_1 x^2 + S_{21}W_3}{W_1 x^2 + W_3}, \\ \hat{S}_3(x, y) = & \frac{S_{32}W_1 x^2 + S_{31}W_2 y^2}{W_1 x^2 + W_2 y^2}. \end{aligned} \quad (27)$$

Similar to the VTI case, we define a relative geometric spreading related function by

$$R = \frac{\cos(\theta)^2 \mathcal{L}_N(x = z \tan(\theta) \cos(\phi), y = z \tan(\theta) \sin(\phi))}{z^2}, \quad (28)$$

and define the dip angle θ and the azimuth ϕ in Figure 5, with the relations

$$\begin{aligned} \theta = & \arctan\left(\frac{\sqrt{x^2 + y^2}}{z}\right), \\ \phi = & \arctan\left(\frac{y}{x}\right). \end{aligned} \quad (29)$$

The Twelve coefficients Q_{ij} , ($i \neq j = 1, 2, 3$) and S_{ij} , ($i \neq j = 1, 2, 3$) in equations 25 and 27, respectively, are computed by fitting with the exact relative geometric spreading (see equation C-2) through the second- and fourth-order derivatives with respect to the dip and azimuth angles by

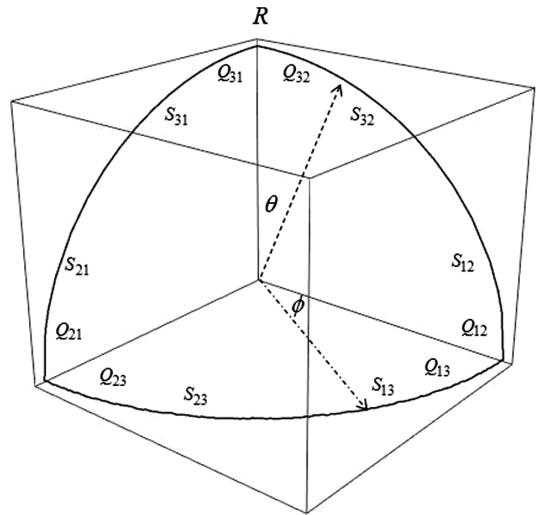


Figure 5. The location of fitting indices Q_{ij} , ($i \neq j = 1, 2, 3$) and S_{ij} , ($i \neq j = 1, 2, 3$) in a homogeneous ORT model.

$$\begin{aligned}
 \left. \frac{\partial^2 R(\phi=0^\circ)}{\partial \theta^2} \right|_{(\theta=0^\circ, 90^\circ)} &\Rightarrow (Q_{32}, Q_{12}); \\
 \left. \frac{\partial^4 R(\phi=0^\circ)}{\partial \theta^4} \right|_{(\theta=0^\circ, 90^\circ)} &\Rightarrow (S_{32}, S_{12}), \\
 \left. \frac{\partial^2 R(\phi=90^\circ)}{\partial \theta^2} \right|_{(\theta=0^\circ, 90^\circ)} &\Rightarrow (Q_{31}, Q_{21}); \\
 \left. \frac{\partial^4 R(\phi=90^\circ)}{\partial \theta^4} \right|_{(\theta=0^\circ, 90^\circ)} &\Rightarrow (S_{31}, S_{21}), \\
 \left. \frac{\partial^2 R(\theta=90^\circ)}{\partial \phi^2} \right|_{(\phi=0^\circ, 90^\circ)} &\Rightarrow (Q_{13}, Q_{23}); \\
 \left. \frac{\partial^4 R(\theta=90^\circ)}{\partial \phi^4} \right|_{(\phi=0^\circ, 90^\circ)} &\Rightarrow (S_{13}, S_{23}). \tag{30}
 \end{aligned}$$

The symmetry of the anelliptic approximation

To calculate 12 coefficients Q_{ij} , ($i \neq j = 1, 2, 3$) and S_{ij} , ($i \neq j = 1, 2, 3$) required for $\hat{Q}_k(x, y)$ and $\hat{S}_k(x, y)$ given in equations 25 and 27, respectively, we focus on each individual symmetry plane sep-

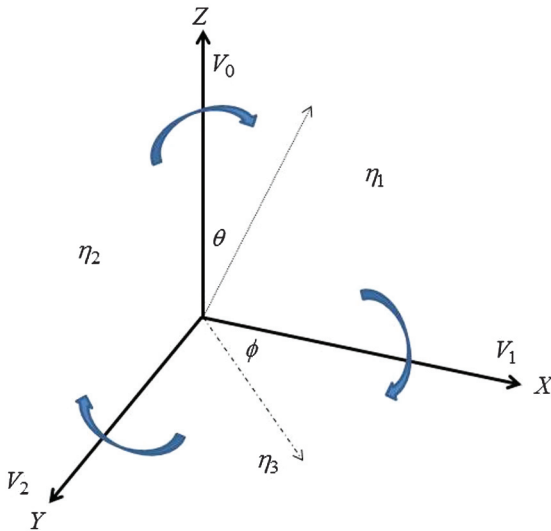


Figure 6. Rotation from $[X, Z]$ symmetry plane to $[X, Y]$ symmetry plane.

Table 2. The corresponding transformation for the model parameters. The anellipticity parameter η_3 can be computed from η_1, η_2 , and η_{xy} , as

$$\eta_3 = \frac{1}{2} \left(\frac{(1+2\eta_1)(1+2\eta_2)}{(1+\eta_{xy})^2} - 1 \right).$$

Plane	Vertical velocity	NMO velocity	Anellipticity parameter	Cross-term anellipticity parameter
$[X, Z]$	V_0	V_{n1}	η_1	$\eta_{xy}^{(1,2)} = \left(\sqrt{\frac{(1+2\eta_1)(1+2\eta_2)}{1+2\eta_3}} - 1 \right)$
$[Y, Z]$	V_0	V_{n2}	η_2	$\eta_{xy}^{(2,1)} = \left(\sqrt{\frac{(1+2\eta_2)(1+2\eta_1)}{1+2\eta_3}} - 1 \right)$
$[X, Y]$	$V_{n1} \sqrt{1+2\eta_1}$	$\frac{V_{n2} \sqrt{1+2\eta_2}}{\sqrt{1+2\eta_3}}$	η_3	$\eta_{xy}^{(1,3)} = \left(\sqrt{\frac{(1+2\eta_1)(1+2\eta_3)}{1+2\eta_2}} - 1 \right)$

arately. When we compute the coefficients in one symmetry plane, similar coefficients for other two symmetry planes can be easily computed by making corresponding changes in indices.

In the $[X, Z]$ symmetry plane, when setting $y = 0$, the anelliptic approximation in equation 21 is similar to the one computed for VTI model. In this symmetry plane, we need to define four coefficients: Q_{32} , Q_{12} , S_{32} , and S_{12} . By taking the second- and fourth-order derivatives of $R(\phi = 0^\circ)$ with respect to the dip angle θ at 0° and 90° , the coefficients Q_{32} , Q_{12} , S_{32} , and S_{12} are computed, as it is shown in Appendix C.

The advantage of anelliptic approximation is its symmetric behavior in different symmetry planes. All required coefficients are computed within one plane and lead to corresponding expressions in the others. The notations for indices in coefficients Q_{ij} and S_{ij} are shown in Figure 5, and changing of indices can be obtained by clockwise rotation of the symmetry frame, as shown in Figure 6.

When we have calculated the coefficients in the $[X, Z]$ symmetry plane, the coefficients in the $[Y, Z]$ and $[X, Y]$ symmetry planes can be easily computed using the transformation rule shown in Table 2. Note that the cross-term anellipticity parameter $\eta_{xy}^{(2,1)}$ defined in the $[Y, Z]$ symmetry plane is the same as $\eta_{xy}^{(1,2)}$ defined in the $[X, Z]$ symmetry plane.

NUMERICAL EXAMPLES

To illustrate the accuracy of our anelliptic approximation, we select a homogeneous ORT model with the following parameters: $t_0 = 1$ s, $V_{n1} = 2$ km/s, $V_{n2} = 2.2$ km/s, $\eta_1 = 0.1$, $\eta_2 = 0.12$, and $\eta_{xy} = 0.2$. We show the relative error from the approximation in Xu et al. (2005) (Figure 7a), indirect rational type approximation (Appendix D; Figure 7b), and our anelliptic approximation (Figure 7c). The form used in Xu et al. (2005) is from the traveltimes derivation based on the rational form moveout approximation (Tsvankin and Thomsen, 1994). One can tell from the comparison that our approximation performs better accuracy, especially along the x - and y -axes, and reaches the maximal error of 0.7% approximately 45° azimuth at the normalized offset $\hat{x} = \hat{y} \approx 1$.

We define a multilayered ORT model with the parameters shown in Table 3 and show the relative error from the approximation in Xu et al. (2005) (Figure 8a), indirect rational type approximation (Appendix D; Figure 8b), and our anelliptic approximation (Figure 8c). The effective model properties for the multilayered ORT model are computed from the Dix-type equations shown in Appendix C. The error surface of the approximation from Xu et al. (2005) and the indirect rational form approximation are more complicated, and their maximal error is larger than our anelliptic approximation. Note that the value of the anisotropy parameters in our paper is much larger than the ones obtained from the field data to make the error from the approximation more visible. In practice, the result from our approximation is more accurate because the anisotropy in practical applicability is weaker.

DISCUSSION

For a multilayered case, the expressions for the relative geometric spreading approximation that we use are computed from the homogeneous model with the effective model parameters com-

Downloaded 01/04/19 to 129.241.69.200. Redistribution subject to SEG license or copyright; see Terms of Use at http://library.seg.org/

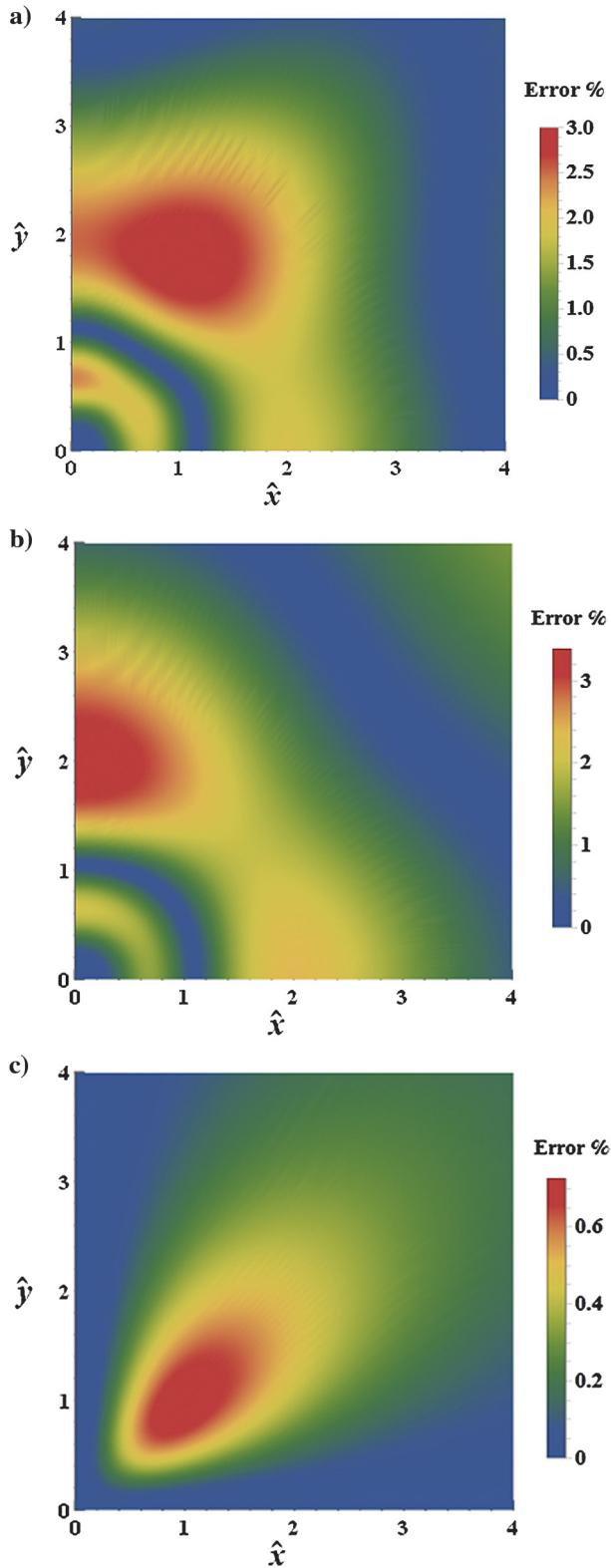


Figure 7. The relative error of the relative geometric spreading for a homogeneous ORT model by using the (a) traveltime-based approximation Xu et al. (2005), (b) indirect rational approximation, and (c) anelliptic approximation.

puted from Dix-type equations (Stovas, 2015). Selecting a horizontal ray for calculation is impossible for ray tracing, which means the assumption for infinite offset limit is not valid anymore, whereas we still using the expression computed from the homogeneous case derived from the infinite offset assumption that explains the lower accuracy compared with homogeneous case. When there is azimuthal variation between the multilayered ORT model, the effective parameters with different azimuthal orientation of the layers are listed in Ravve and Koren (2017) and Koren and Ravve (2017).

Our anelliptic form resembling equations in Sripanich and Fomel (2015) are defined for the group velocity inverse for VTI and ORT models. The difference is that they define the anelliptic form for group velocity inverse first, computing the coefficients from fitting, then convert it to the traveltime approximation, whereas our anelliptic form approximation is defined for relative geometric spreading, then by using the converted relation to obtain the coefficients. The converted relation is needed for the anelliptic form traveltime and geometric spreading approximation because there is no asymptotic behavior for traveltime or geometric spreading at infinite offset that can be used for fitting.

The tricky part of our approximation is that we use the relative geometric spreading related functions r (VTI) and R (ORT) to derive the coefficients used in approximation. This function has no physical meaning but is used for a fitting technique. There is a simple relation between the function r (or R) and corresponding term \mathcal{L}_N . The form of this function is similar to the group velocity inverse in VTI and ORT models.

For example, in the VTI case, function r is very similar to $1/V(\theta)^2$, where V is the group velocity and θ is the group angle. The traveltime and offset are given as

$$t = \frac{z}{V(\theta) \cos(\theta)}, \quad x = z \tan(\theta). \quad (31)$$

The converted relation applied for traveltime and relative geometric spreading is shown by

$$\begin{aligned} \frac{1}{V_{\text{group}}^2} &= \frac{\cos(\theta)^2}{z^2} t^2(x = z \tan(\theta)), \\ r &= \frac{\cos(\theta)^2}{z^2} \mathcal{L}_N(x = z \tan(\theta)), \end{aligned} \quad (32)$$

where z represents the depth. We do not have the value for depth because the offset x in the geometric spreading approximation \mathcal{L}_N is represented by $x = z \tan(\theta)$, which cancels the depth factor z in the denominator, keeping only the variable θ used for fitting.

The relative geometric spreading \mathcal{L}_N is shown by the form of traveltime derivative with respect to the offset in equation 4. Substituting the traveltime form in equation 31 and taking the derivative with respect to the offset x gives

Table 3. The model parameters in a multilayered ORT model.

Layer	z (km)	V_0 (km/s)	V_{n1} (km/s)	V_{n2} (km/s)	η_1	η_2	η_{xy}
1	0.25	1.5	1.65	1.8	0.05	0.08	0.2
2	0.75	1.8	2	2.2	0.1	0.1	0.18
3	1	2	2.2	2.15	0.08	0.12	0.22

$$\mathcal{L}_N = \frac{V^2 z}{\cos(\theta)^2} \sqrt{\frac{V}{(V - V' \cot(\theta))(2V'^2 + V(V - V''))}}. \quad (33)$$

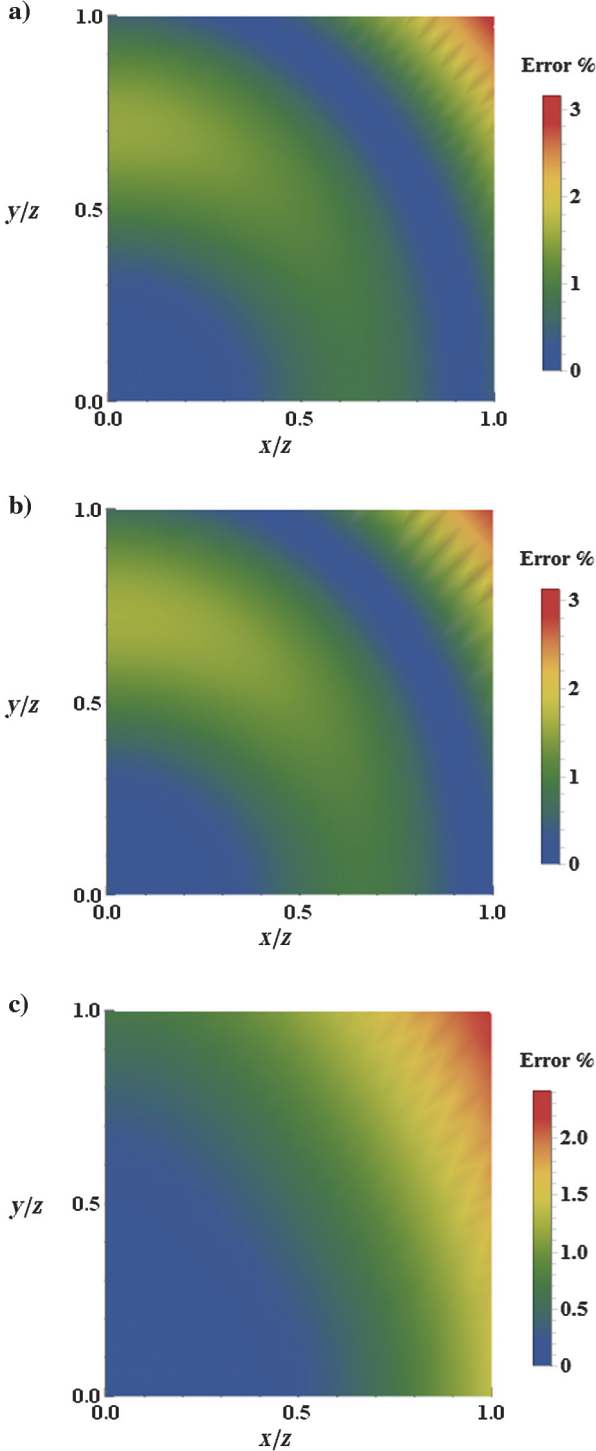


Figure 8. The relative error of the relative geometric spreading for a multilayered ORT model by using the (a) traveltime-based approximation Xu et al. (2005), (b) indirect rational approximation, and (c) anelliptic approximation.

The function r can be represented in the group velocity and its derivatives with respect to the group angle

$$\begin{aligned} r &= \frac{\mathcal{L}_N \cos(\theta)^2}{z^2} \\ &= \frac{V^2}{z} \sqrt{\frac{V}{(V - V' \cot(\theta))(2V'^2 + V(V - V''))}}. \end{aligned} \quad (34)$$

For anelliptic form traveltime approximation (Sripanich and Fomel, 2015), $1/V^2(\theta)$ is the one used for fitting process at $\theta = 0^\circ$ and 90° . However, for our anelliptic form geometric spreading, the function r (combination of group velocity and its derivatives) given in equation 34 is the one used for the fitting process, which is much more complete compared with the traveltime case ($1/V^2(\theta)$).

The beauty of the anelliptic approximation is that we use the properties only on the three symmetry planes; therefore, the behaviors in three planes are all symmetric. It is convenient to get the coefficients in other planes by proper rotation on the index after obtaining the coefficients in one symmetry plane.

For anelliptic traveltime approximation for an ORT model (Sripanich and Fomel, 2015), when we focus on one symmetry plane, the approximation converges to the one defined for a VTI model. For anelliptic relative geometric spreading approximation, the situation is different, and the approximation does not converge to the VTI counterpart (Appendix A) or any of symmetry planes due to the different number of parameters. This happens due to the mixed derivatives entering the equation for geometric spreading (equation 4). The NMO velocities V_{n1} , V_{n2} and cross-term anellipticity parameters are presented in all equations defined either in $[X, Z]$ or $[Y, Z]$ symmetry planes.

To reduce the relative geometric spreading from ORT to VTI cases, the following reduction in parameters is required:

$$\begin{aligned} V_{n2} &= V_{n1} = V_n, \\ \eta_2 &= \eta_1 = \eta, \\ \eta_{xy} &= 2\eta, \\ \eta_3 &= 0. \end{aligned} \quad (35)$$

CONCLUSION

We propose an anelliptic form approximation for the relative geometric spreading in a homogeneous VTI and ORT media under the acoustic anisotropy assumption. All the coefficients in the approximation are calculated by fitting with the exact parametric solution within the symmetry planes. Compared with the GMA form approximation, our anelliptic approximation is more accurate for larger offset in a homogeneous VTI model. Due to symmetric behavior, the coefficients of the approximation in ORT model can be easily obtained after computing the coefficients in one symmetry plane and applying the required rotation for the other. The form of the anelliptic approximation is simpler, whereas the traveltime-based counterparts are algebraically complicated. In the numerical examples, one can see that compared with the traveltime-based approximations, our anelliptic form approximation is more accurate for homogeneous and multilayered ORT models.

ACKNOWLEDGMENTS

We would like to thank the China Scholarship Council and the Rose Project for the financial support. Y. Sripanich thanks the sponsors of the Texas Consortium for Computational Seismology for financial support. Y. Sripanich was also additionally supported by the Statoil Fellows Program at the University of Texas at Austin. We also thank I. Ravve, P. Golikov, and A. Gassiyev for their comments and helpful suggestions.

APPENDIX A

THE COEFFICIENTS q_1 , q_3 , s_1 , AND s_3 OF THE ANELLIPTIC APPROXIMATION FOR A TRANSVERSELY ISOTROPIC MEDIUM WITH A VERTICAL SYMMETRY AXIS

The function r in VTI model is defined in equation 12, the derivatives of r with respect to the group angle θ at zero offset are

$$\begin{aligned} \frac{\partial^2 r}{\partial \theta^2 (\theta=0)} &= \frac{q_3}{t_0 \sqrt{1+2\eta}} \frac{t_0 V_n^2}{z^2}, \\ \frac{\partial^4 r}{\partial \theta^4 (\theta=0)} &= \frac{2s_3((1+2\eta)t_0^4 V_n^4 - \sqrt{1+2\eta} q_3 t_0^2 V_n^2 z^2 + 3\sqrt{1+2\eta}(1-q_1-2q_3)z^4) - 3(q_3-1)^2 z^4}{6(1+2\eta)s_3 t_0^2 V_n^2 z^2}. \end{aligned} \quad (\text{A-1})$$

The derivatives of r with respect to the group angle θ at infinite offset are

$$\begin{aligned} \frac{\partial^2 r}{\partial \theta^2 (\theta=\pi/2)} &= -\frac{1}{t_0 \sqrt{1+2\eta}} \frac{t_0 V_n^2 q_1}{z^2}, \\ \frac{\partial^4 r}{\partial \theta^4 (\theta=\pi/2)} &= \frac{-3(1+2\eta)^{3/2} t_0^4 V_n^4 (1+q_1^2 - 2(1+q_3)s_1 - 2q_1(1-2s_1)) - 2(1+2\eta)q_1 s_1 t_0^2 V_n^2 z^2 + 2\sqrt{1+2\eta} s_1 z^4}{6(1+2\eta)s_1 t_0 z^4}. \end{aligned} \quad (\text{A-2})$$

By fitting with the exact form, the coefficients q_1 , q_3 , s_1 , and s_3 are given by

$$\begin{aligned} q_1 &= \sqrt{1+2\eta}(1+8\eta+12\eta^2), \\ q_3 &= \sqrt{1+2\eta}(1+8\eta), \\ s_1 &= \frac{(1+\eta(9+4\eta(15+2\eta(23+3\eta(11+6)))) - \sqrt{1+2\eta}(1+2\eta)(1+6\eta)}{(1+9\eta(1+2\eta)^3(1+4\eta)) - \sqrt{1+2\eta}(1+8\eta)(1+3\eta)}, \\ s_3 &= \frac{(1+9\eta+48\eta^2+64\eta^3) - \sqrt{1+2\eta}(1+8\eta)}{(1+9\eta+54\eta^2+72\eta^3) - \sqrt{1+2\eta}(1+8\eta-12\eta^2)}. \end{aligned} \quad (\text{A-3})$$

In the elliptical case ($\eta = 0$, $q_1 = q_3 = 1$, and $s_1 = s_3 = 9/13$), the function r becomes

$$r = \frac{\cos(\theta)^2 t_0 V_n^2}{z^2} + \frac{\sin(\theta)^2}{t_0}. \quad (\text{A-4})$$

APPENDIX B

THE EFFECTIVE MODEL PARAMETERS FOR THE MULTILAYERED TRANSVERSELY ISOTROPIC AND ORTHORHOMBIC MEDIA

The effective model parameters from the multilayered model are computed from traveltimes (high frequency) and from

upscaling (low frequency). The computation in our paper is computed from dynamic ray tracing, so the traveltimes parameters are used. The Dix-type equation is derived from the Dix (1955) inversion that is estimating the individual layer parameters from the recorded reflections on seismic seismogram for the horizontally layered medium.

To apply approximation in equation 8 computed from the homogeneous model for a multilayered VTI medium, the effective parameters by using the Dix-type equations are shown by

$$\begin{aligned} \tilde{t}_0 &= \sum_{j=1}^m t_{0j}, \\ \tilde{V}_n &= \sqrt{\frac{\sum_{j=1}^m V_{nj}^2 t_{0j}}{\tilde{t}_0}}, \\ \tilde{\eta} &= \frac{1}{8} \left(\frac{\sum_{j=1}^m (1+8\eta_j) V_{nj}^4 t_{0j}}{\tilde{V}_n^4 \tilde{t}_0} - 1 \right), \quad m=1, \dots, 3. \end{aligned} \quad (\text{B-1})$$

The exact form of relative geometric spreading in a multilayered VTI case is computed from the summation as shown below:

$$\begin{aligned} x(p) &= \sum_{j=1}^m \frac{p t_{0j} V_{nj}^2}{(1-2\eta_j p^2 V_{nj}^2)^{3/2} \sqrt{1-(1+2\eta_j) p^2 V_{nj}^2}}, \\ \mathcal{L}_N &= \sum_{j=1}^m \frac{t_{0j} V_{nj}^2 \sqrt{1+4\eta_j p^2 V_{nj}^2 - 6\eta_j(1+2\eta_j) p^4 V_{nj}^4}}{(1-2\eta_j p^2 V_{nj}^2)^2 (1-(1+2\eta_j) p^2 V_{nj}^2)}, \quad m=1, \dots, 3. \end{aligned} \quad (\text{B-2})$$

It is computed by summing for each individual layers (equation B-2) that explains why the relative error does not go to zero for large offset-depth ratio.

Similar to the multilayered VTI case, the effective properties used in multilayered ORT model are computed from Dix-type equations (Stovas, 2015):

$$\begin{aligned} \tilde{t}_0 &= \sum_{j=1}^m t_{0j}, \\ \tilde{V}_{n1} &= \sqrt{\frac{\sum_{j=1}^m V_{n1j}^2 t_{0j}}{\tilde{t}_0}}, \\ \tilde{V}_{n2} &= \sqrt{\frac{\sum_{j=1}^m V_{n2j}^2 t_{0j}}{\tilde{t}_0}}, \\ \tilde{\eta}_1 &= \frac{1}{8} \left(\frac{\sum_{j=1}^m (1+8\eta_{1j}) V_{n1j}^4 t_{0j}}{\tilde{V}_{n1}^4 \tilde{t}_0} - 1 \right), \\ \tilde{\eta}_2 &= \frac{1}{8} \left(\frac{\sum_{j=1}^m (1+8\eta_{2j}) V_{n2j}^4 t_{0j}}{\tilde{V}_{n2}^4 \tilde{t}_0} - 1 \right), \\ \tilde{\eta}_{xy} &= \frac{1}{4} \left(\frac{\sum_{j=1}^m (1+4\eta_{xyj}) V_{n1j}^2 V_{n2j}^2 t_{0j}}{\tilde{V}_{n1}^2 \tilde{V}_{n2}^2 \tilde{t}_0} - 1 \right), \quad m=1, \dots, 3. \end{aligned} \quad (\text{B-3})$$

The exact relative geometric spreading in multilayered ORT is computed by summation for individual layers by parametric equations 15, 16, and 17 as shown below:

$$\begin{aligned} x(p_x, p_y) &= \sum_{j=1}^m p_x F_2'^2 \frac{V_{n1j}^2 t_{0j}}{f_1'^{1/2} f_2'^{3/2}}, \\ y(p_x, p_y) &= \sum_{j=1}^m p_y F_1'^2 \frac{V_{n2j}^2 t_{0j}}{f_1'^{1/2} f_2'^{3/2}}, \\ \mathcal{L}_N &= \sum_{j=1}^m t_{0j} V_{n1j} V_{n2j} \frac{F_1' F_2'}{f_2'^2 f_1'} \sqrt{f_m'}, \quad m = 1, \dots, 3, \quad (\text{B-4}) \end{aligned}$$

where

$$\begin{aligned} F_1' &= 1 - p_x^2 V_{n1j}^2 (2\eta_{1j} - \eta_{xyj}), \\ F_2' &= 1 - p_y^2 V_{n2j}^2 (2\eta_{2j} - \eta_{xyj}), \\ f_1' &= 1 - (1 + 2\eta_{1j}) p_x^2 V_{n1j}^2 - (1 + 2\eta_{2j}) p_y^2 V_{n2j}^2 + ((1 + 2\eta_{1j}) \\ &\quad \times (1 + 2\eta_{2j}) - (1 + \eta_{xyj})^2) p_x^2 p_y^2 V_{n1j}^2 V_{n2j}^2, \\ f_2' &= 1 - 2\eta_{1j} p_x^2 V_{n1j}^2 - 2\eta_{2j} p_y^2 V_{n2j}^2 + (4\eta_{1j} \eta_{2j} - \eta_{xyj}^2) p_x^2 p_y^2 V_{n1j}^2 V_{n2j}^2, \\ f_m' &= 1 + 4\eta_{1j} p_x^2 V_{n1j}^2 + 4\eta_{2j} p_y^2 V_{n2j}^2 - 6\eta_{1j} (1 + 2\eta_{1j}) \\ &\quad \times p_x^4 V_{n1j}^4 - 6\eta_{2j} (1 + 2\eta_{2j}) p_y^4 V_{n2j}^4 \\ &\quad + 2(8\eta_{1j} \eta_{2j} - \eta_{xyj} (3 + 5\eta_{xyj})) p_x^2 p_y^2 V_{n1j}^2 V_{n2j}^2 \\ &\quad - 6(1 + 2\eta_{1j}) (4\eta_{1j} \eta_{2j} - \eta_{xyj}^2) p_x^4 p_y^2 V_{n1j}^4 V_{n2j}^2 - 6(1 + 2\eta_{2j}) \\ &\quad \times (4\eta_{1j} \eta_{2j} - \eta_{xyj}^2) p_x^2 p_y^4 V_{n1j}^2 V_{n2j}^4 \\ &\quad + 9((1 + 2\eta_{1j})(1 + 2\eta_{2j}) - (1 + \eta_{xyj})^2) (4\eta_{1j} \eta_{2j} - \eta_{xyj}^2) \\ &\quad \times p_x^4 p_y^4 V_{n1j}^4 V_{n2j}^4. \quad (\text{B-5}) \end{aligned}$$

APPENDIX C

THE COEFFICIENTS OF THE ANELLIPTIC APPROXIMATION FOR ORTHORHOMBIC MODEL IN $[X, Z]$ PLANE

The coefficients of the anelliptic approximation defined in the symmetry plane of the ORT model are not the same as those computed for the VTI case (Appendix A). Due to the presence of mixed derivatives in equation 14 or equation 15, all ORT model parameters are entering the equations defined in any of symmetry planes. However, with the use of the cross-term anelliptic parameter η_{xy} , the number of parameters can be reduced to five. For the $[X, Z]$ symmetry plane, these parameters are V_0 , V_{n1} , V_{n2} , η_1 , and η_{xy} .

To calculate the coefficients in the anelliptic form approximation in the $[X, Z]$ plane, we set $y = 0$ in the approximation given in equation 21. Only the $[X, Z]$ plane coefficients Q_{32} , Q_{12} , S_{32} , and S_{12} remain in the approximation.

We introduce the relative geometric spreading related function R ($R = \cos(\theta)^2 \mathcal{L}_N / z^2$), where θ is the dip group angle to the vertical axis and z is the depth, we get the second- and fourth-order derivatives of R with respect to θ as follows:

$$\begin{aligned} \frac{\partial^2 R}{\partial \theta^2} (\theta=0) &= \frac{V_{n2}}{V_{n1} t_0} \left(\frac{(1 + \eta_{xy}) Q_{32}}{(1 + 2\eta_1)^{3/2}} - \frac{V_{n1}^2 t_0^2}{z^2} \right), \\ \frac{\partial^4 R}{\partial \theta^4} (\theta=0) &= \frac{V_{n2}}{6(1 + 2\eta_1)^{7/2} S_{32} t_0^3 V_{n1}^3 z^2} \left(-3\sqrt{1 + 2\eta_1} (1 + \eta_{xy})^2 \right. \\ &\quad \times (Q_{32} - 1)^2 z^4 + 2S_{32} ((1 + 2\eta_1)^{7/2} t_0^4 V_{n1}^4 \\ &\quad - (1 + 2\eta_1)^2 (1 + \eta_{xy}) Q_{32} t_0^2 V_{n1}^2 z^2 \\ &\quad \left. + 3\sqrt{1 + 2\eta_1} (1 + \eta_{xy})^2 (1 + Q_{12} - 2Q_{32}) z^4 \right), \\ \frac{\partial^2 R}{\partial \theta^2} (\theta=\pi/2) &= \frac{V_{n2}}{V_{n1} t_0} \left(\frac{V_{n1}^2 t_0^2 Q_{12}}{z^2} - \frac{1 + \eta_{xy}}{(1 + 2\eta_1)^{3/2}} \right), \\ \frac{\partial^4 R}{\partial \theta^4} (\theta=\pi/2) &= \frac{V_{n2}}{6(1 + 2\eta_1)^{7/2} S_{12} t_0 V_{n1} z^4} (-3(1 + 2\eta_1)^3 \\ &\quad (1 + Q_{12}^2 - 2(1 + Q_{32}) S_{12} + 2Q_{12} (2S_{12} - 1)) t_0^4 V_{n1}^4 \\ &\quad - 2(1 + 2\eta_1)^{3/2} (1 + \eta_{xy}) Q_{12} S_{12} t_0^2 V_{n1}^2 z^2 \\ &\quad + 2(1 + \eta_{xy})^2 S_{12} z^4). \quad (\text{C-1}) \end{aligned}$$

By fitting with the exact form, the coefficients: Q_{12} , Q_{32} , S_{32} , and S_{12} are given as

$$\begin{aligned} Q_{12} &= \sqrt{1 + 2\eta_1} (1 + 8\eta_1 + 6\eta_1 \eta_{xy}), \\ Q_{32} &= \frac{(1 + 2\eta_1)^{3/2} (1 + 6\eta_1 + \eta_{xy})}{1 + \eta_{xy}}, \\ S_{12} &= \frac{e_1 + \sqrt{1 + 2\eta_1} e_2}{e_3 + \sqrt{1 + 2\eta_1} e_4}, \\ S_{32} &= \frac{f_1 + \sqrt{1 + 2\eta_1} f_2}{f_3 + \sqrt{1 + 2\eta_1} f_4}, \quad (\text{C-2}) \end{aligned}$$

where

$$\begin{aligned} e_1 &= (1 + \eta_{xy}) (1 + \eta_1 (9 + 6\eta_{xy} + 2\eta_1 (4 + 3\eta_{xy})) \\ &\quad \times (6 + 8\eta_1 + 3\eta_{xy} + 6\eta_1 \eta_{xy})), \\ e_2 &= -(1 + \eta_{xy}) (1 + \eta_1 (8 + 6\eta_{xy})), \\ e_3 &= (1 + \eta_{xy}) (1 + 9\eta_1 (1 + 6\eta_1 + 8\eta_1^2) (1 + \eta_{xy})^2), \\ e_4 &= -1 - \eta_{xy} + 2\eta_1 (-4 + 6\eta_1 - \eta_{xy} (13 + 6\eta_{xy})), \\ f_1 &= 144\eta_1^5 + (1 + \eta_{xy})^2 + 3\eta_1 (1 + \eta_{xy}) (3 + \eta_{xy}) + 24\eta_1^4 (11 + 2\eta_{xy}) \\ &\quad + 6\eta_1^2 (10 + \eta_{xy} (8 + \eta_{xy})) + 4\eta_1^3 (46 + \eta_{xy} (20 + \eta_{xy})), \\ f_2 &= -(1 + 2\eta_1) (1 + \eta_{xy}) (1 + 6\eta_1 + \eta_{xy}), \\ f_3 &= 9\eta_1 (1 + 2\eta_1)^3 (1 + 4\eta_1) + (1 + \eta_{xy})^2, \\ f_4 &= -(1 + \eta_{xy}) (1 + \eta_{xy} + 2\eta_1 (4 + 12\eta_1 - \eta_{xy} (5 + 3\eta_{xy}))). \quad (\text{C-3}) \end{aligned}$$

By setting $\eta_1 = \eta$ and $\eta_{xy} = 2\eta$, the coefficients defined in equation C-2 become equivalent to those defined in equation A-3 for VTI model, $Q_{12} = q_1$, $Q_{32} = q_3$, $S_{12} = s_1$, and $S_{32} = s_3$.

Due to the symmetric behavior in the symmetry plane in ORT model, the other coefficients in the approximation can be easily obtained by corresponding changes in indices from the computed the

coefficients in one symmetry plane (see the transformation form in Table 2). The coefficients (Q_{21} , Q_{31} , S_{21} , and S_{31}) defined in the $[Y, Z]$ plane and the coefficients (Q_{23} , Q_{13} , S_{23} , and S_{13}) defined in the $[X, Y]$ plane are obtained from the $[X, Z]$ plane coefficients (Q_{32} , Q_{12} , S_{32} , and S_{12}) by setting ($\eta_1 \rightarrow \eta_2$) and ($\eta_1 \rightarrow \eta_3$, $\eta_{xy} \rightarrow \eta_{xy}^{13}$), respectively. Note that $\eta_{xy} \equiv \eta_{xy}^{12} = \eta_{xy}^{21}$.

APPENDIX D

THE INDIRECT RATIONAL FORM APPROXIMATION FOR RELATIVE GEOMETRIC SPREADING IN AN ORT MODEL

A rational form similar to the Vasconcelos and Tsvankin (2006) approximation for the traveltine in ORT model is defined by

$$T_{\text{RA}}^2 = A_{00} + A_{20}x^2 + A_{02}y^2 + \frac{A_{40}x^4 + A_{22}x^2y^2 + A_{04}y^4}{1 + (B_{20}x^2 + B_{02}y^2)}, \quad (\text{D-1})$$

where the coefficients A_{00} , A_{20} , A_{02} , A_{40} , A_{22} , and A_{04} computed from the Taylor series at zero offset are given by

$$A_0 = t_0^2, A_{20} = \frac{1}{V_{n1}^2}, A_{02} = \frac{1}{V_{n2}^2},$$

$$A_{40} = -\frac{2\eta_1}{t_0^2 V_{n1}^4}, A_{04} = -\frac{2\eta_2}{t_0^2 V_{n2}^4}, A_{22} = -\frac{2\eta_{xy}}{t_0^2 V_{n1}^2 V_{n2}^2}. \quad (\text{D-2})$$

The remaining coefficients B_{20} and B_{02} are computed by the infinite offset limit shown as

$$B_{20} = \frac{1 + 2\eta_1}{t_0^2 V_{n1}^2}, \quad B_{02} = \frac{1 + 2\eta_2}{t_0^2 V_{n2}^2}. \quad (\text{D-3})$$

The indirect (traveltine-based) rational form approximation for relative geometric spreading is given by the derivatives of traveltine approximation in equation D-1 with respect to the offsets given by

$$\mathcal{L}_N = \left(\left(\frac{\partial^2 T_{\text{RA}}}{\partial x^2} \frac{\partial^2 T_{\text{RA}}}{\partial y^2} \right) - \left(\frac{\partial^2 T_{\text{RA}}}{\partial x \partial y} \frac{\partial^2 T_{\text{RA}}}{\partial y \partial x} \right) \right)^{-1/2}. \quad (\text{D-4})$$

Note that the indirect rational form approximation in equation D-4 is algebraically complicated due to the second-order derivatives.

REFERENCES

Alkhalifah, T., 1998, Acoustic approximations for processing in transversely isotropic media: *Geophysics*, **63**, 623–631, doi: [10.1190/1.1444361](https://doi.org/10.1190/1.1444361).
 Alkhalifah, T., 2003, An acoustic wave equation for orthorhombic anisotropy: *Geophysics*, **68**, 1169–1172, doi: [10.1190/1.1598109](https://doi.org/10.1190/1.1598109).
 Červený, V., 2001, *Seismic ray theory*: Cambridge University Press.
 Dix, C. H., 1955, Seismic velocities from surface measurements: *Geophysics*, **20**, 68–86, doi: [10.1190/1.1438126](https://doi.org/10.1190/1.1438126).

Fomel, S., 2004, On anelliptic approximations for qP velocities in VTI media: *Geophysical Prospecting*, **52**, 247–259, doi: [10.1111/j.1365-2478.2004.00413.x](https://doi.org/10.1111/j.1365-2478.2004.00413.x).
 Fomel, S., and A. Stovas, 2010, Generalized nonhyperbolic moveout approximation: *Geophysics*, **75**, no. 2, U9–U18, doi: [10.1190/1.3334323](https://doi.org/10.1190/1.3334323).
 Fowler, P. J., 2003, Practical VTI approximations: A systematic anatomy: *Journal of Applied Geophysics*, **54**, 347–367.
 Golikov, P., and A. Stovas, 2012, Accuracy comparison of nonhyperbolic moveout approximations for qP-waves in VTI media: *Journal of Geophysics and Engineering*, **9**, 428–432, doi: [10.1088/1742-2132/9/4/428](https://doi.org/10.1088/1742-2132/9/4/428).
 Golikov, P., and A. Stovas, 2013, Moveout-based geometrical spreading approximation in TTI media: 75th Annual International Conference and Exhibition, EAGE, Extended Abstracts, Tu P0614.
 Grechka, V., and I. Tsvankin, 1999a, 3-D moveout velocity analysis and parameter estimation for orthorhombic media: *Geophysics*, **64**, 820–837, doi: [10.1190/1.1444593](https://doi.org/10.1190/1.1444593).
 Grechka, V., and I. Tsvankin, 1999b, 3-D moveout inversion in azimuthally anisotropic media with lateral velocity variation: Theory and a case study: *Geophysics*, **64**, 1202–1218, doi: [10.1190/1.1444627](https://doi.org/10.1190/1.1444627).
 Koren, Z., and I. Ravve, 2017, Fourth-order normal moveout velocity in elastic layered orthorhombic media. Part 2: Offset-azimuth domain: *Geophysics*, **82**, no. 3, C113–C132, doi: [10.1190/geo2016-0222.1](https://doi.org/10.1190/geo2016-0222.1).
 Ravve, I., and Z. Koren, 2017, Fourth-order normal moveout velocity in elastic layered orthorhombic media. Part 1: Slowness-azimuth domain: *Geophysics*, **82**, no. 3, C91–C111, doi: [10.1190/geo2015-0621.1](https://doi.org/10.1190/geo2015-0621.1).
 Schoenberg, M., and K. Helbig, 1997, Orthorhombic media: Modeling elastic wave behavior in a vertically fractured earth: *Geophysics*, **62**, 1954–1974, doi: [10.1190/1.1444297](https://doi.org/10.1190/1.1444297).
 Sripanich, Y., and S. Fomel, 2015, On anelliptic approximations for qP velocities in transversely isotropic and orthorhombic media: *Geophysics*, **80**, no. 5, C89–C105, doi: [10.1190/geo2014-0534.1](https://doi.org/10.1190/geo2014-0534.1).
 Stovas, A., 2015, Azimuthally dependent kinematic properties of orthorhombic media: *Geophysics*, **80**, no. 6, C107–C122, doi: [10.1190/geo2015-0288.1](https://doi.org/10.1190/geo2015-0288.1).
 Stovas, A., 2017, Geometrical spreading in orthorhombic media: *Geophysics*, **83**, this issue, doi: [10.1190/geo2016-0710.1](https://doi.org/10.1190/geo2016-0710.1).
 Stovas, A., and B. Ursin, 2009, Improved geometric-spreading approximation in layered transversely isotropic media: *Geophysics*, **74**, no. 5, D85–D95, doi: [10.1190/1.3158051](https://doi.org/10.1190/1.3158051).
 Tsvankin, I., 1997, Anisotropic parameters and P-wave velocity for orthorhombic media: *Geophysics*, **62**, 1292–1309, doi: [10.1190/1.1444231](https://doi.org/10.1190/1.1444231).
 Tsvankin, I., 2012, Seismic signatures and analysis of reflection data in anisotropic media: SEG.
 Tsvankin, I., and L. Thomsen, 1994, Nonhyperbolic reflection moveout in anisotropic media: *Geophysics*, **59**, 1290–1304, doi: [10.1190/1.1443686](https://doi.org/10.1190/1.1443686).
 Ursin, B., 1990, Offset-dependent geometrical spreading in a layered medium: *Geophysics*, **55**, 492–496, doi: [10.1190/1.1442860](https://doi.org/10.1190/1.1442860).
 Ursin, B., and K. Hokstad, 2003, Geometrical spreading in a layered transversely isotropic medium with vertical symmetry axis: *Geophysics*, **68**, 2082–2091, doi: [10.1190/1.1635062](https://doi.org/10.1190/1.1635062).
 Vasconcelos, I., and I. Tsvankin, 2006, Non-hyperbolic moveout inversion of wide-azimuth P-wave data for orthorhombic media: *Geophysical Prospecting*, **54**, 535–552, doi: [10.1111/j.1365-2478.2006.00559.x](https://doi.org/10.1111/j.1365-2478.2006.00559.x).
 Xu, S., and A. Stovas, 2017, Direct geometrical spreading approximation in anisotropic media: 79th Annual International Conference and Exhibition, EAGE, Extended Abstracts, Tu P8 13.
 Xu, S., A. Stovas, and Q. Hao, 2016, Perturbation-based moveout approximations in anisotropic media: *Geophysical Prospecting*, **65**, 1218–1230, doi: [10.1111/1365-2478.12480](https://doi.org/10.1111/1365-2478.12480).
 Xu, X., and I. Tsvankin, 2006, Anisotropic geometrical-spreading correction for wide-azimuth P-wave reflection: *Geophysics*, **71**, no. 5, D161–D170, doi: [10.1190/1.2335615](https://doi.org/10.1190/1.2335615).
 Xu, X., and I. Tsvankin, 2007, A case study of azimuthal AVO analysis with anisotropic spreading correction: *The Leading Edge*, **26**, 1552–1561, doi: [10.1190/1.2821942](https://doi.org/10.1190/1.2821942).
 Xu, X., and I. Tsvankin, 2008, Moveout-based geometrical-spreading correction for PS-waves in layered anisotropic media: *Journal of Geophysics and Engineering*, **5**, 195–202, doi: [10.1088/1742-2132/5/2/006](https://doi.org/10.1088/1742-2132/5/2/006).
 Xu, X., I. Tsvankin, and A. Pech, 2005, Geometrical spreading of P-waves in horizontally layered, azimuthally anisotropic media: *Geophysics*, **70**, no. 5, D43–D53, doi: [10.1190/1.2052467](https://doi.org/10.1190/1.2052467).
 Zhou, H., and G. A. McMechan, 2000, Analytical study of the geometrical spreading of P-waves in a layered transversely isotropic medium with vertical symmetry axis: *Geophysics*, **65**, 1305–1315, doi: [10.1190/1.1444822](https://doi.org/10.1190/1.1444822).